

EPR observation of cathodically-generated radical anions of colchicides and isocolchicides, and a comparison with the radical anions of troponoids. A general rationalization of the spin-density distribution in these systems

Marino Cavazza,^{a,*} Calogero Pinzino,^b Lucio Pardi,^c Lamberto Nucci,^a Francesco Pergola^{a,†} and Francesco Pietra^d

^aDipartimento di Chimica e Chimica Industriale, Università di Pisa, via Risorgimento 35, I-56100 Pisa, Italy

^bIstituto per i Processi Chimico-Fisici (IPCF-CNR), via Moruzzi 1, I-56124 Pisa, Italy

^cINFM and Dipartimento di Fisica, Università di Pisa, Piazza Torricelli, I-56100 Pisa, Italy

^dVia della Fratta 9, I-55100 Lucca, Italy

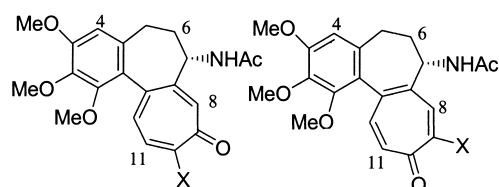
In memory of Sergio Santucci

Received 31 July 2002; revised 10 September 2002; accepted 3 October 2002

Abstract—Cathodic reduction of 10-ethylthiocolchicide (**2**), 9-ethoxyisocolchicide (**3**), 9-methylthioisocolchicide (**4**), 9-*n*-butylthioisocolchicide (**5**), and 9-phenylthioisocolchicide (**6**) at a platinum electrode in DMF under N₂ gave the corresponding radical anions for which EPR spectra were recorded. Voltammetric analysis of these compounds revealed a reversible wave at minimum scan rate 0.1–0.5 V s⁻¹. Hyperfine coupling constants (hfcc) for these radical anions—assigned by spectral simulation and DFT calculations of electron spin densities—are highest at the position adjacent to the carbonyl group. Decreasingly small hfccs were assigned, in the given order, to the γ and β positions with respect to the carbonyl group. This trend—which is only marginally affected by oxygen, amino, and sulfur substituents—can be qualitatively rationalized on the basis of classical resonance structures. These afford stability to the system in diminishing order for the unpaired electron at the α, γ, or β position with respect to the cycloheptatrienone carbonyl group, which corresponds to conjugation of the unpaired electron through three, two, or one C=C bonds, respectively. Similar conclusions apply to a variety of substituted troponoids. © 2002 Elsevier Science Ltd. All rights reserved.

1. Introduction

Recently we have revisited the cathodic behavior of 10-methoxycolchicide (=colchicine, **1**, Chart 1), detecting an intermediate radical anion for which the EPR spectrum was recorded.¹ Theoretical interest in, and possible



1 X = OMe
2 X = SEt

3 X = OEt
4 X = SMe
5 X = S-*n*-Bu
6 X = SPh

Chart 1.

Keywords: cycloheptatrienones; electrochemistry; electron spin resonance.

* Corresponding author; e-mail: marcav@dcc.unipi.it

† Deceased 30 April, 2002.

relevance to cellular functions of this radical anion,¹ has stimulated us to examine the radical anions of both a sulfur substituted colchicide, **2**, and a variety of isocolchicinoids (**3–6**, Chart 1), the latter being a class that is not known to display cellular activity.² We show here that the distribution of the unpaired electron on the radical anions of both the colchicinoids and the isocolchicinoids can be rationalized on the basis of classical resonance structures. This rationalization can also be extended to the radical anions of a variety of troponoids (**7–18**, Chart 2).

2. Results and discussion

2.1. Cathodic behavior

Voltammetric analysis of dilute (ca. 10⁻⁴ M), N₂-flushed, DMF/*n*-Bu₄NClO₄ solutions of 10-ethylthiocolchicide (**2**), 9-ethoxyisocolchicide (**3**), 9-methylthioisocolchicide (**4**), 9-*n*-butylthioisocolchicide (**5**), and 9-phenylthioisocolchicide (**6**) at room temperature at a Pt cathode revealed a single voltammetric wave, reversible at scan rates of

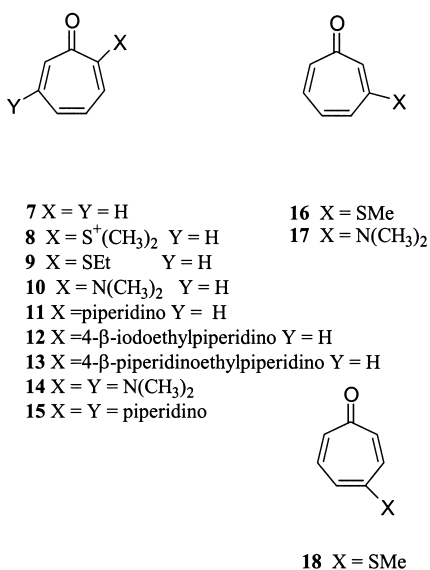


Chart 2.

0.1–0.5 V s⁻¹ (Table 1). On increasing the substrate concentration, faster scan rates were needed in order to observe a reversible wave. The same behavior was observed for colchicine (**1**),¹ which required a 10-fold faster scan rate than **3** in order to achieve reversibility. Therefore, the radical anions from compounds **2**–**6** are more stable than the colchicine (**1**) radical anion. The same conclusion was arrived at from a kinetic investigation of decaying EPR signals, as shown in Section 2.4. The peak and half wave reduction potentials have similar values in both series (Table 1), the largest deviations being observed for 9-ethoxyisocolchicidide (**3**) and 9-phenylthioisocolchicidide (**6**), which are more cathodic and less cathodic, respectively, than colchicine (**1**).

The cathodic behavior of chlorotroponoids,³ methoxytroponoids,⁴ and a variety of other substituted troponoids,⁵ proved similar to that for **2**–**6** in regard to the voltammetric-wave form and peak potential. Representative data for 2-dimethylsulfoniotropone (**8**) and 2-dimethylaminotropone (**10**) are reported in Table 1, together with those for the parent member, troponone (**7**). The minimum scan rate

Table 1. Data for the cathodic reduction of colchicinoids **1**, **2**, isocolchicinoids **3**–**6**, and troponoids **7**, **8**, and **10**

Compound	Cyclic voltammetry		<i>E</i> _{1/2} (V vs SCE)
	Scan rate (V s ⁻¹)	<i>E</i> _p (V vs SCE)	
1	1	-1.63	-1.60 ^a
2	0.2	-1.62	-1.56
3	0.1	-1.80	-1.77
4	0.5	-1.60	-1.56
5	0.5	-1.59	-1.55
6	0.5	-1.45	-1.43
7	0.51, ^b 0.05 ^c	-1.34	
8	0.75 ^b	-0.65	
10	0.75 ^b	-1.73	

At a Pt cathode, N₂ flushed DMF, 0.1 M TBAP, compd 4 × 10⁻⁴ mol L⁻¹, room temperature, reversible processes with a single voltammetric wave.

^a From Ref. 1.

^b Compound 10⁻³ mol L⁻¹.

^c Compound 5 × 10⁻⁵ mol L⁻¹.

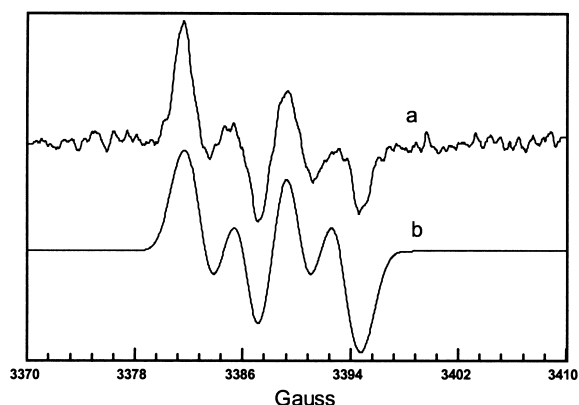


Figure 1. EPR spectrum of the radical anion obtained from cathodic reduction of **2** in DMF at room temperature: (a) experimental spectrum, (b) simulated spectrum.

sufficient for **7**, **8**, and **10** to display reversibility is of the order of that observed for **3** at a 10-fold higher concentration (Table 1). This implies that the radical anions of **7**, **8** and **10** have higher stability than the radical anion of **3**. The same conclusion was arrived at by comparing the kinetics for the decaying radical anions of colchicinoids **4**–**6** (Section 2.4) with those reported for troponone,⁶ and other troponoids,^{3–5} which showed decreasing stability in the order **10** > 2-fluotroponone > 4-methoxytroponone ≅ 3-methoxytroponone ≅ 2-chlorotroponone > **8** > **7** > **9** > **7** > **14** > 4-chlorotroponone > 3-chlorotroponone > 3-tosyloxytroponone > 4-tosyloxytroponone > 2-tosyloxytroponone ≅ 2-bromotroponone ≅ 2-iodotroponone ≅ 4-bromotroponone ≅ 4-iodotroponone.⁵

2.2. Radical anions of colchicinoids and isocolchicinoids

On the basis of the above electrochemical indications, reduction of 10-ethylthioisocolchicidide (**2**) and the isocolchicinoids **3**–**6**, 10⁻³ mol L⁻¹ in dry DMF, was carried out directly in the EPR spectrometer cavity by the methodology already used for colchicine (**1**).¹

Like in the latter case,¹ the EPR spectrum of 10-ethylthioisocolchicidide (**2**) radical anion is also characterized by a quartet of sextets (Fig. 1(a)). Simulation of the recorded spectrum¹ gave two major hyperfine coupling constants (hfcc), one twice as large as the other one, 7.11 and 3.14 G, alongside minor hfccs, 1.51 G, for coupling to a single proton, and 0.80 G, for coupling with two magnetically equivalent protons (Fig. 1(b)). By analogy with the radical anion of colchicine (**1**), the largest coupling can be assigned to H-8, the second largest one to H-12, and the third largest one to H-11. The smallest coupling, 0.80 G, most likely involves the methylene group at sulfur (Table 2).

The EPR spectra of the isocolchicinoid radical anions (Figs. 2(a)–5(a)) are also characterized by two major hfccs, one twice as large as the other one for **3**, as for **1** and **2**. In contrast, however, the ratio is 3:1 for **4**–**6**. Spectral simulation of the experimental spectra⁷ (Figs. 2(b)–5(b)) furnished the values for the two major couplings, while minor couplings were also revealed—two for the radical anion of **3**, and three for the radical anions of **4**–**6** (Table 2). By analogy with the radical anions of both the colchicinoids **1**, **2** and the troponoids (Table 3),^{3–5} the largest coupling for

Table 2. Hyperfine coupling constants for colchicinoids **1**, **2** and isocolchicinoids **3–6**

Position	1	2	3	4	5	6
4	0.48, ^a 0.48 ^b					
6			−0.4 ^c			
7				1.29, ^a 1.23 ^c	1.27, ^a 1.20 ^c	1.65, ^a 1.73 ^c
8	8.9, ^a −9.2 ^b	7.11, ^a −6.95 ^c	3.17, ^a −3.08 ^c	2.69, ^a −2.53 ^c	2.56, ^a −2.20 ^c	2.55, ^a −2.53 ^c
9-OCH ₂ CH ₃			1.18, ^a −1.05 ^c			
9-OCH ₂ CH ₃			0.42 ^a			
9-SMe				0.36, ^a 0.30 ^c		
9-SCH ₂ C ₃ H ₇					1.08, ^a −1.05 ^c	
9-SC ₆ H ₅						1.63, ^a −1.50 ^c
10-OMe	0.75, ^a 0.84 ^b					
10-SCH ₂ CH ₃		0.80, ^a −0.91 ^c				
11	0.49, ^a 0.59 ^b	1.51, ^a −1.37 ^c	7.39, ^a −7.20 ^c	7.35, ^a −7.60 ^c	7.33, ^a −7.50 ^c	7.53, ^a −7.60 ^c
12	4.3, ^a −5.0 ^b	3.14, ^a −3.03 ^c	0.51 ^c	0.60, ^a 0.64 ^c	0.54, ^a 0.50 ^c	0.48, ^a −0.51 ^c

^a Experimental.^b UHF/UMP2/6-31** calculations from Ref. 1.^c DFT calculations (this work).

3–6 can be assigned to H-11. In the lack of deuterium labeled compounds, all other assignments had to rely on calculations only. In this regard, density functional theory (DFT)-based calculations (see Section 4) were performed for the radical anions of **2** and **3–6**, furnishing the electron spin densities at the carbon atoms and, through Fermi contact interactions, the hfcc for the corresponding hydrogen atoms. The map of electron spin density distribution is displayed in Fig. 6 for the radical anion of **2** and Fig. 7 for

that of **3**. The latter is also a good representation for the electron spin density distribution for the radical anions of **4–6**. This confirms the above assignment of the largest and second largest couplings, 7.11 and 3.14 G, to H-8 and H-12 for the radical anion of **2**, respectively, and suggests that the weaker couplings, 1.51 and 0.80 G, are to be attributed to H-11 and CH₂S, respectively (Table 2).

DFT calculations for the radical anions in the isocolchicinoid

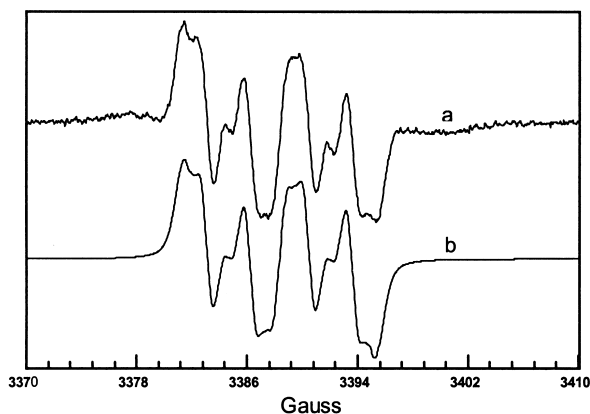
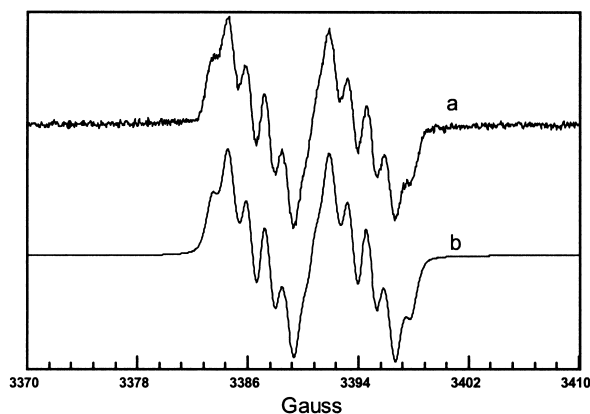
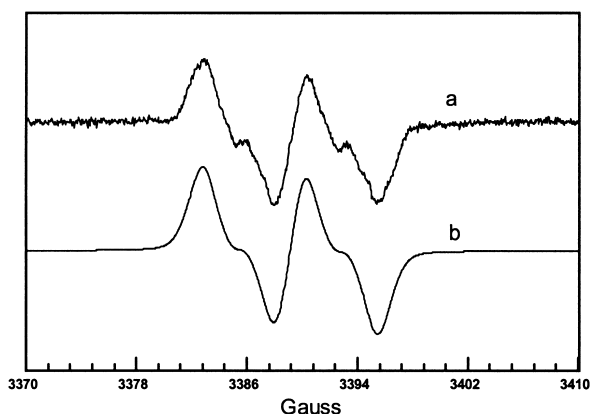
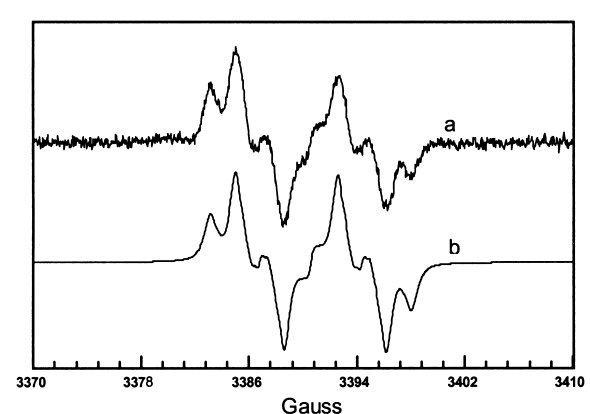
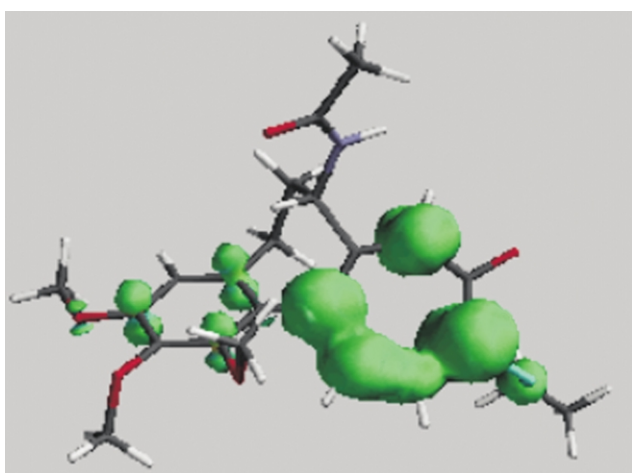
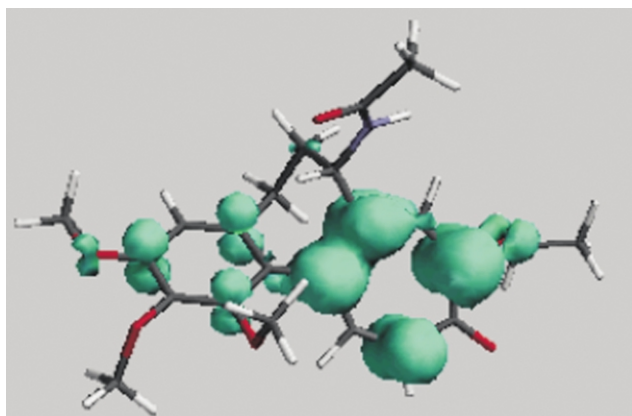
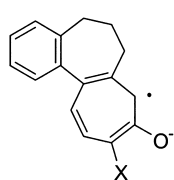
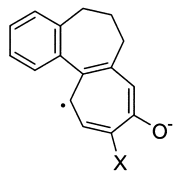
**Figure 2.** EPR spectrum of the radical anion of **3**: (a) experimental, (b) simulated.**Figure 4.** EPR spectrum of the radical anion of **5**: (a) experimental, (b) simulated.**Figure 3.** EPR spectrum of the radical anion of **4**: (a) experimental, (b) simulated.**Figure 5.** EPR spectrum of the radical anion of **6**: (a) experimental, (b) simulated.

Table 3. Hyperfine coupling constants for troponoids 7–18

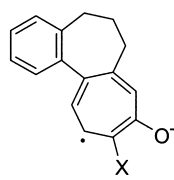
Position	7 ^a	8	9	10	11	12	13	14	15	16	17	18
2	8.58									7.12 ^b	7.7 ^b	8.5 ^b
3	0.1	0.0, ^b 1.77 ^c	0.0, ^b 0.07 ^c	0.0 ^b	0.0 ^b	0.0 ^b	0.0 ^b	0.0 ^b	0.0 ^b			0.0 ^b
4	5.0	5.0, ^b 5.81 ^c	3.5, ^b 4.80 ^c	4.0 ^b	4.6 ^b	5.1 ^b	4.9 ^b	4.1 ^b	3.5 ^b	3.76 ^b	5.9 ^b	
5	5.0	5.0, ^b 6.15 ^c	6.1, ^b 7.50 ^c	4.8 ^b	4.6 ^b	5.1 ^b	4.9 ^b	4.8 ^b	4.1 ^b	4.48 ^b	4.1 ^b	5.3 ^b
6	0.1	1.6, ^b 1.36 ^c	0.0, ^b 2.00 ^c	0.7 ^b	0.0 ^b	0.0 ^b	0.0 ^b	0.0 ^b	0.0 ^b	0.0 ^b	0.8 ^b	0.0 ^b
7	8.58	8.8, ^b 7.90 ^c	9.0, ^b 10.8 ^c	8.2 ^b	7.9 ^b	8.5 ^b	8.2 ^b	8.0 ^b	5.9 ^b	6.84 ^b	8.1 ^b	8.5 ^b
2-SCH ₂ CH ₃ 2-N(CH ₃) ₂			0.86 ^b		0.7 ^b				0.7 ^b			

^a Data from Ref. 6.^b Experimental.^c SCF MO (CNDO/2) calculations.**Figure 6.** Calculated spin density surface (0.002 electron a.u.⁻³) of the radical anion of 2.**Figure 7.** Calculated spin density surface (0.002 electron a.u.⁻³) of the radical anion of 3.

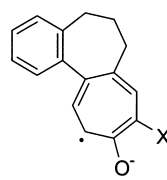
A



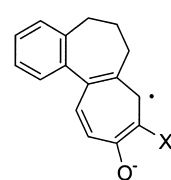
B



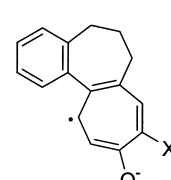
C

Chart 3.

A



B



C

Chart 4.

series, 3–6, support the above experimental assignment of the largest coupling to H-11 and suggest attributing to H-8 the second largest coupling and to H-12 the 0.60 G coupling for 4, 0.54 G for 5, 0.48 G for 6, and the vanishingly small coupling for 3 (Table 2).

The observed distribution of the spin density on both the colchicinoids and the isocolchicinoids is amenable to a qualitative rationalization based on classical resonance structures. As to the colchicinoids, the largest hfcc at H-8 is linked to the greatest stability of the unpaired electron at that position, indicated by a conjugated set of three C=C bonds ending in the negatively charged oxygen (structure A, Chart 3). Only two C=C bonds are interposed for H-12 (structure B, Chart 3), accounting for the second largest hfcc. Similarly, for the isocolchicinoids the resonance structure A of Chart 4 attributes to H-11 the largest hfcc (three C=C set). Although for both H-8 and H-12 the conjugation set with the negatively charged oxygen bears one C=C bond only (structures B and C, Chart 4), position 8 (structure B, Chart 4) may be seen in conjugation with the arene ring; this may account for a larger coupling at H-8 than H-12.

2.3. Radical anions of troponoids

The isotropic hfccs for troponoids were assigned with the aid of a simulation program and SCF-MO CNDO/2 calculations,⁸ like for the chlorotropones.³ In the case of 8 and 9 this assignment was further supported by deuterium labeling. As in the case of colchicinoids and isocolchicinoids, the isotropic-hfcc trend for the radical anions of the troponoids can be qualitatively interpreted on the basis of classical resonance structures. The unpaired electron at the α carbon, as in structure A of Chart 5, benefits from the most extensive delocalization, from the α carbon to the negatively charged oxygen atom, through three C=C bonds. Stabilization stems from only two C=C bonds for

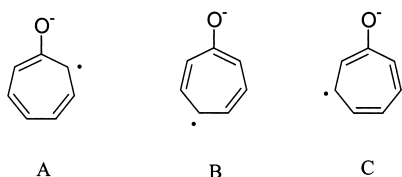


Chart 5.

the unpaired electron at the γ carbon (Chart 5, B). For the unpaired electron at the β -position (Chart 5, C) just a single C=C bond affords delocalization. This rationalizes the decreasing hfcc absolute values in the order $\alpha > \gamma \gg \beta$. Within this trend, the particular hfcc values are only marginally affected by the nature of the substituents X and Y (Table 3),^{3–5} which gives strong support to the above resonance-structure-based rationalization.

2.4. Kinetic data for the decay of radical anions

EPR kinetic measurements were carried out for the radical anions of the isocolchicinoids **4**–**6** both during cathodic formation and disappearance once the electric current flow was interrupted. From the trend of the EPR signals (Fig. 8)—which fit first order kinetic equations—both processes can be assumed to be kinetically first order. Starting with ca. 10^{-3} M solutions of the isocolchicinoids in dry DMF at room temperature, we obtained $k_1 = 1.0 \times 10^{-4} \text{ s}^{-1}$ and $k_2 = 6.0 \times 10^{-2} \text{ s}^{-1}$ for **4**, $k_1 = 1.3 \times 10^{-4} \text{ s}^{-1}$ and $k_2 = 5.9 \times 10^{-2} \text{ s}^{-1}$ for **5**, and $k_1 = 8.1 \times 10^{-5} \text{ s}^{-1}$ and $k_2 = 6.2 \times 10^{-2} \text{ s}^{-1}$ for **6**, where k_1 and k_2 are the first-order rate coefficients for the formation and the decay of the radical anion, respectively. Under the caveat that determination of the kinetic order in a wide range of initial radical-anion concentrations could not be performed, and that k_2 might be a pseudo first-order rate coefficient if the solvent acts as a protonating species in the rate limiting process, our kinetic data indicate that the half-life of the radical anions of both the colchicinoids and the isocolchicinoids is in the order of 10 s, which is much shorter than the half-life of tropone radical anion, ca. 900 s.⁶

3. Conclusions

Our study has shown that the decreasing order of spin density $\alpha > \gamma \gg \beta$ (for positions relative to the carbonyl group) in the radical anions of troponoids does not fully hold for the isocolchicinoids. In fact for **3**–**6**, the above β rule, valid for the troponoids and for both **1** and **2**, holds for position 12 only. Substantial spin density at position 8 may be attributed to extra conjugation of the unpaired electron with the benzene ring. This notwithstanding, the radical anions of both colchicinoids and isocolchicinoids are more labile than the tropone radical anion. This puzzle is resolved by assuming that kinetic and thermodynamic factors do not run in parallel.

4. Experimental

4.1. General procedures

Apparatus and techniques for the electrochemical measure-

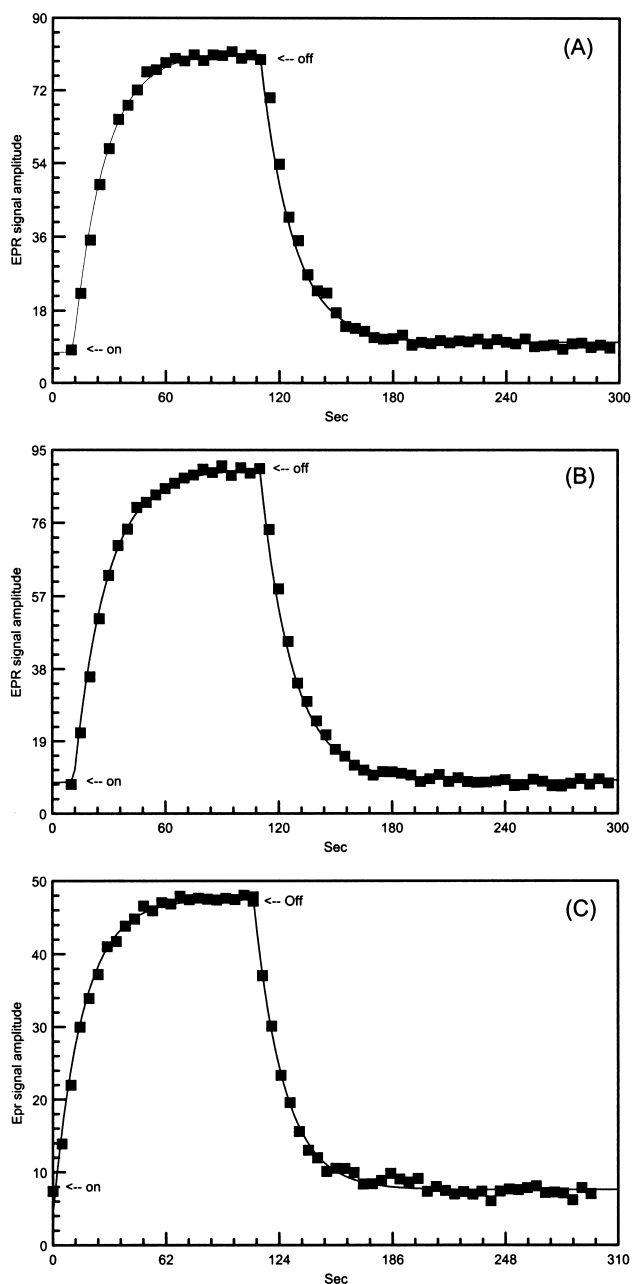


Figure 8. Experimental (square) and computed (line) EPR kinetics for the radical anion of **4** (A), **5** (B) and **6** (C) during cathodic formation (electric current flow on) and disappearance (electric current flow off) in DMF solution at room temperature.

ments were previously described.¹ DMF was distilled from, and stored on, molecular sieves under N_2 . The following compounds were synthesized according to the literature: **2**,⁹ **3**,¹⁰ **4**,¹¹ **5** and **6**,¹² **8**,¹³ **9**,¹⁴ **10**,¹⁵ **11**–**13**,¹⁶ **13**, **14**, and **17**,¹⁷ and **16** and **18**.³

4.2. EPR measurements

EPR spectra and the time evolution of the amplitude of the highest line in each spectrum (EPR kinetics) were taken with a Varian E 112 EPR spectrometer. This was interfaced to a IPC 610/P566C industrial grade Advantech computer by means of a home made data-acquisition system. The latter consisted of an acquisition board capable of acquiring

up to 500000 12-bit samples for second, including 32-bit add to memory—thus giving on-line signal averaging¹⁸—and a software package specially designed for EPR experiments.¹⁹ The EPR spectra were taken as described previously.¹

4.3. Computational details

Full optimization of the molecular geometry of the radical anions, and calculation of the electron spin density distribution and surfaces, were carried out using the UNIX version of the Spartan 5.1.3 computer program,²⁰ running on a Digital/Compaq workstation. DFT data were obtained by adopting the p-BP86 scheme that uses the functional proposed by Becke²¹ and the Perdew correlation functional, which adopts the DN** base-function set, appropriate for isotropic hfcc calculations of split-valence-plus-polarization quality. The influence of the solvent was corrected through semi-empirical extrapolations.^{22,23}

Acknowledgements

We thank MURST and CNR, Roma, for financial support.

References

1. Cavazza, M.; Nucci, L.; Pannocchia, E.; Pardi, L.; Pergola, F.; Pinzino, C.; Pietra, F. *Tetrahedron* **1999**, *55*, 11601–11608, due to a misprint, the reduction potential of colchicine reported on p 11602, -1.79 V (vs SHE), should read -1.60 V (vs SCE) -1.4 V (vs SHE).
2. Capraro, H.-G.; Brossi, A. *The Alkaloids*, Brossi, Ed.; Academic: New York, 1984; Vol. XXIII.
3. (a) Cavazza, M.; Colombini, M. P.; Martinelli, M.; Nucci, L.; Pardi, L.; Pietra, F.; Santucci, S. *J. Am. Chem. Soc.* **1977**, *99*, 5997–6002. (b) Martinelli, M.; Nucci, L.; Pardi, L.; Pietra, F.; Santucci, S. *Tetrahedron Lett.* **1975**, 2089–2090.
4. Festa, C.; Nucci, L.; Pietra, F.; Moresco, A. M.; Pardi, L.; Santucci, S. *J. Chem. Soc., Perkin Trans. 2* **1976**, 180–182.
5. Colombini, M. P. Doctoral Thesis, University of Pisa, 1976.
6. Ikegami, Y.; Watanabe, H.; Seto, S. *Bull. Chem. Soc. Jpn* **1972**, *45*, 1976–1978.
7. Duling, D. R. *J. Magn. Reson. B* **1994**, *104*, 105–110.
8. Pople, J. A.; Beveridge, D. L. *Approximate Molecular Orbital Theory*. McGraw-Hill: New York, 1970.
9. Cavazza, M.; Pietra, F. *J. Chem. Soc., Perkin Trans. 1* **1995**, 2657–2661.
10. Cavazza, M.; Pietra, F. *Tetrahedron* **1998**, *54*, 14059–14064.
11. Velluz, L.; Muller, G. *Bull. Soc. Chim. Fr.* **1955**, 198.
12. Cavazza, M.; Pietra, F. *Z. Naturforsch.* **1996**, *51b*, 1347–1351.
13. Cavazza, M.; Veracini, C. A.; Pietra, F. *Tetrahedron Lett.* **1975**, 2085–2086.
14. Veracini, C. A.; Pietra, F. *J. Chem. Soc., Chem. Commun.* **1974**, 623–624.
15. Nozoe, T.; Seto, S.; Tokeda, H.; Morosoiva, S.; Matsumoto, K. *Sci. Repts. Tohoku Univ.* **1952**, *1*, 126.
16. Biggi, G.; Del Cima, F.; Pietra, F. *J. Am. Chem. Soc.* **1972**, *94*, 4700–4707.
17. Ricciarelli, B.; Cabrino, R.; Del Cima, F.; Pietra, F. *J. Chem. Soc., Chem. Commun.* **1974**, 723–724.
18. Ambrosetti, R.; Ricci, D. *Rev. Sci. Instrum.* **1991**, *62*, 2281–2283.
19. Pinzino, C.; Forte, C. ESR-ENDOR, ICQEM-CNR Pisa, Italy, 1992.
20. *Spartan*, version 5.1.3; Wavefunction, Inc.: 18401 Von Karman Avenue, Suite 370 Irvine, CA 92612, USA.
21. Becke, A. D. *J. Chem. Phys.* **1993**, *98*, 1372–1377.
22. Fortunelli, A.; Salvetti, O. *J. Mol. Struct. (Theochem)* **1993**, *287*, 89–92.
23. Fortunelli, A. *Int. J. Quantum Chem.* **1994**, *52*, 97–108.